Article

Journal of
Nanoscience and Nanotechnology
Vol. 18, 4428–4438, 2018
www.aspbs.com/jnn

Characterization of Articaine-Loaded Poly(ε-caprolactone) Nanocapsules and Solid Lipid Nanoparticles in Hydrogels for Topical Formulations

Nathalie Ferreira Silva de Melo[1,*], Estefânia Vangelie Ramos Campos[2], Michelle Franz-Montan[3], Eneida de Paula[4], Camila Morais Gonçalves da Silva[4], Cíntia Rodrigues Maruyama[2], Tatiane Pasquoto Stigliani[5], Renata de Lima[5], Daniele Ribeiro de Araújo[6], and Leonardo Fernandes Fraceto[2]

[1] *Department of Immunology and Molecular Biology, São Leopoldo Mandic Research Institute, Campinas, 13045755, SP, Brazil*
[2] *Department of Environmental Engineering, São Paulo State University, Sorocaba, 18180000, SP, Brazil*
[3] *Department of Physiological Sciences, Piracicaba Dental School, University of Campinas, Piracicaba, 13414018, SP, Brazil*
[4] *Department of Biochemistry, State University of Campinas, Campinas, 13083862, SP, Brazil*
[5] *Department of Biotechnology, University of Sorocaba, Sorocaba, 18023-000, SP, Brazil*
[6] *Federal University of ABC, Santo André, 09210580, SP, Brazil*

This work describes the development of poly-ε-caprolactone nanocapsules (PCL-NC) and solid lipid nanoparticles (SLN) aiming delivery for articaine (ATC), in order to improve its chemical stability in semi-solid preparations looking forward their use for skin delivery. The nanoparticles were characterized by size, polydispersity index, and pH. Cellular viability was evaluated using the MTT test and the *in vitro* release kinetics was determined using a two-compartment model. The hydrogels with nanoparticle suspensions were characterized considering their rheological aspects and *in vitro* permeation across artificial membranes. Colloidal stability was satisfactory, since the formulations did not present major alterations during 120 days. High ATC encapsulation was achieved (78% for PCL-NC and 65% for SLN). The release profile of PCL-NC-ATC was slower, compared to the free molecule and SLN-ATC. MTT experiments showed the nanosystems were capable to increase cellular viability compared with free ATC. The hydrogels showed good consistency, homogeneity, and stability and presented pseudoplastic behavior with thixotropy, improving drug efficacy in clinical applications. The gel based on PCL-NC showed faster onset of activity and flux of 35.68 ± 1.98 $\mu g/cm^2/h$, which then continued for up to 8 h. This study opens up prospects for employment of nanoparticulate systems for modified release of ATC.

Keywords: PCL Nanocapsules, Solid Lipid Nanoparticles, Semisolid Formulation, Hydrogel, Topical Anesthetics, Articaine.

1. INTRODUCTION

The development of nanocarriers to overcome the common problem of poor drug solubility in water is currently one of the main themes in pharmaceutical research.[1,2] Micro-and nanoencapsulation techniques are among the approaches that have attracted the most attention. Polymeric nanocapsules (NC) used as carriers of drugs or other active molecules are vesicle-like structures (polymeric shell and an oily core), where the compounds are dispersed in the core or trapped in the polymeric layer.[1] Solid lipid nanoparticles (SLN) are matrix structures constituted of biodegradable solid lipids, stabilized using emulsifiers to disperse the active compounds in the lipid matrix.[3] The properties of biodegradability and biocompatibility are very important for polymers and lipids used in medical practice. Suitable compounds include poly(ε-caprolactone) (PCL), a polyester employed in the preparation of NC, and glyceryl tripalmitate, used to produce SLN capable of being loaded with drugs.[4]

*Author to whom correspondence should be addressed.

 1533-4880/2018/18/4428/011 doi:10.1166/jnn.2018.15235

The amino-amide local anesthetic articaine (ATC) presents particular characteristics able to influence its metabolism and half-life. The presence in the molecule of a thiophene ring and additional ester group increases anesthetic potency as well enhances diffusion within the tissues.[5,6] Some adverse effects are reported of ATC administration, such as prolonged and permanent paresthesia. This complication seems to have been associated with inferior alveolar and lingual nerve blockade.[5,7]

A technique that has been shown to be able to promote the desired effects of drugs is their modified release using carrier systems. The development of such systems for ATC is of considerable interest because the drug displays superior performance, compared to other anesthetics of the same class, and has been increasingly used in dental and topical procedures.[8] In this way, the ATC encapsulation (hydrochloride salt) in other nanocarrier systems such as alginate/chitosan nanoparticles[9] and multilamellar liposomes[10] have been shown to reduce the toxicity of the anesthetic and a slower release profile was achieved. Also, liposomal formulation proved to be an alternative to infiltrative anesthesia in uninflamed tissues.[10] Despite of ATC evokes low intensity inflammatory effects,[11] some important clinical side effects (such as anaphylaxis or atypical reactions) have been reported.[12]

For this reason, drug–drug-delivery systems have been topically applied because they present some advantages such as bioadhesion, prolonged permanence at the site of application and greater chemical stability and reduced toxicity, resulting in improved therapeutic efficacy.[13] However, the preformulation phase is vital to evaluate the compatibility of the pharmaceutical adjuvants and, particularly, to develop new products and optimize the existing formulations.[14]

A wide range of raw materials are available for the preparation of topical gels and the selection of a suitable substance for use in the development of a new formulation is based on considerations regarding to colloidal stability, release kinetics and effectiveness of the active principle that it is intended to incorporate. It is therefore important to evaluate the physicochemical properties and measure the drug release, as necessary prerequisites for the purposes of quality control.[15]

In this work, PCL-NC and SLN loaded with ATC (in its uncharged form) were manufactured after screening the preparation conditions and optimizing the composition of the formulation, since only few reports in the literature have been considered the development of delivery systems for ATC.[9,10,16,17] and they did not intend to topical use. It is noteworthy that there is not yet commercially available a formulation for topical use of ATC local anesthetic. Then, our objectives were to characterize the nanoparticles suspensions, assess their colloidal stability, and compare the *in vitro* release profiles of free and encapsulated ATC in both nanoparticulated systems. Besides, we also extended our investigation for the development of hydrogels formulations with a view to their use for skin local anesthesia.

2. MATERIALS AND METHODS

2.1. Materials

ATC hydrochloride was kindly donated by DFL Industry (Rio de Janeiro, Brazil). Poly(ε-caprolactone) (PCL, 70–90 kDa), capric/caprylic triglycerides, glyceryl tripalmitate, propylene glycol, polyvinyl alcohol (PVA, 30–70 kDa) and methylparaben were purchased from Sigma-Aldrich Chem. Co. (St. Louis, MO, USA). The Aristoflex® AVC was acquired from Clariant (Muttenz, Swiss). Acetone and chloroform (analytical grade) were obtained from LabSynth (Diadema, SP, Brazil). Acetonitrile (HPLC grade) was obtained from Tedia Chemicals (Fairfield, OH, USA). DMEM (Dulbecco's Modified Eagle Medium), colchicine, fetal bovine serum, penicillin, and streptomycin sulfate were purchased from Cultilab (Campinas, SP, Brazil). The water used was purified and filtered through a 0.22 μm membrane. Other reagents employed were spectroscopic or analytical grade.

2.2. Production of the Free Base Form of ATC

The free base form of ATC was obtained as the hydrochloride salt. The neutral form was employed as the nanocarriers used here are quite applied to non-ionized drug. One gram of ATC hydrochloride was dissolved in deionized water and the pH value was adjusted to 9 using NaOH solution. The aqueous phase was extracted three times with ethyl acetate. The organic phase was dried with sodium sulfate, filtered, and evaporated to yield oil that was crystallized by storage at −18 °C. The ATC crystals were examined by Fourier transform infrared spectroscopy (FTIR), differential scanning calorimetry (DSC), and high performance liquid chromatography (HPLC), and compared with the hydrochloride salt.[18]

2.3. Preparation of PCL Nanocapsules

The PCL nanocapsules were prepared according to the method described by Campos et al.,[19] changing only the drug employed. ATC (200 mg) and capric/caprylic triglycerides (200 mg) were dissolved in acetone (10 mL) and mixed with chloroform (20 mL) containing the PCL polymer (400 mg). The pre-emulsion was produced using ultrasonication (1 min, 100 W). Aqueous phase containing PVA (50 mL) was then added and the mixture was also ultrasonicated (8 min, 100 W). The resulting suspension was placed in a rotary evaporator to remove the solvents and concentrate to 10 mL. The final ATC concentration was 20 mg/mL. These nanoparticles have been previously characterized in another study.[16]

2.4. Preparation of Solid Lipid Nanoparticles

Preparation of the SLN employed the method described by de Oliveira et al.,[20] also changing the drug used. Briefly,

glyceryl tripalmitate (250 mg) and ATC (200 mg) were dissolved in chloroform (5 mL) and mixed with 30 mL of aqueous phase containing PVA (375 mg). This mixture was sonicated (5 min, 40 W) to produce an emulsion, which was then submitted to Ultra Turrax homogenization (7 min/18000 rpm). After this, the organic solvent was eliminated by evaporation under low pressure and the final volume was 10 mL, giving a final ATC concentration of 20 mg/mL.

2.5. Photon Correlation Spectroscopy (PCS)

The average diameter and polydispersity index (PI) of the nanoparticles were determined using PCS. The PI was obtained from the size distribution of the nanoparticles. The measurements were performed at 25 °C using a Zeta-Sizer Nano ZS 90 analyzer (Malvern Instruments, UK), with an angle of 90°, after dilution of the samples in purified water. The results were expressed as the average of three analyses (mean ± SD).[16, 21, 22] The average diameter and polydispersion of the nanoparticles contained in the gels were also determined using the same PCS technique. About one gram of gel containing nanoparticles was dispersed in purified water and the size and PI values were measured under the same conditions already mentioned.

2.6. Transmission Electron Microscopy (TEM)

A JEOL 1200 EXII TEM (JEOL Ltd., Japan) operated at 80 kV was used to analyze the morphology of the nanoparticles.[23] Prior to analysis, the samples were diluted, contrasted using uranyl acetate (2%), deposited onto copper grids coated with a carbon film, and dried at ambient temperature.

2.7. Encapsulation Efficiency

The amount of ATC encapsulated was determined by a method combining ultrafiltration and centrifugation.[16, 17, 22] The suspensions were centrifuged in ultrafiltration devices (Amicon® 10 kDa MWCO) (Millipore, Billerica, MA, USA). ATC was then quantified in the ultrafiltrate using a Varian ProStar HPLC instrument (Agilent Technologies, Santa Clara, CA, USA) fitted with a PS210 isocratic pump and a UV-Vis detector. A Gemini® C_{18} column NX 5μ C_{18} 110 Å, 150 × 4.6 mm (Phenomenex, Torrance, CA, USA) was maintained at 35 °C. The mobile phase was composed of 0.02 mol/L sodium dihydrogen phosphate (adjusted to pH 3.0 with phosphoric acid) and acetonitrile, at a ratio of 88:12 (v/v), with a flow rate of 2 mL/min. The mobile phase was filtered and degassed prior to use. The sample injection volume was 100 μL and the detector wavelength was 273 nm.[17]

The ATC was determined after dilution of the suspensions with acetonitrile, which caused solubilization of the system and released the drug into solution. Quantification of ATC employed a validated analytical curve, as described previously.[17]

The ATC encapsulation efficiency (*EE%*) was calculated from the difference between the total and free ATC concentrations, measured in the suspension and ultrafiltrate, respectively, according to Eq. (1):

$$EE\% = \frac{W_{\text{free}}}{W_{\text{total}}} \times 100 \quad (1)$$

where W_{free} is the mass of free ATC in solution and W_{total} is the total mass of ATC present in the suspension.

2.8. Differential Scanning Calorimetry (DSC)

Portions (2 mg) of each sample (ATC, PCL polymer, glyceryl tripalmitate, empty NC, NC with ATC, empty SLN, SLN with ATC, and physical mixtures) were analyzed using a TA Instruments Q20 (New Castle, DE, USA) differential scanning calorimeter equipped with a cooler system and calibrated using indium. The samples were transferred to sealed aluminum pans and heated from −10 to 300 °C, at a rate of 10 °C/min, under a nitrogen flow rate (50 mL/min) and using an empty pan as the Ref. [23].

2.9. Stability of the Suspensions

The chemical stability of the PCL-NC and SLN suspensions containing ATC was evaluated by measurements of the pH of the suspensions as a function of time, using a pH meter (Tecnal, Brazil). Changes in pH values may indicate degradation of the polymer and lipid. The colloidal stability was followed over time using measurements of average diameter and polydispersity index. The stability trials were continued for a period of 120 days, during which the formulations were stored at ambient temperature.[17, 22]

2.10. Cellular Viability

The experiments employing the MTT (a yellow tetrazole) reduction test were carried out with Balb-c 3T3 cells maintained in continuous culture in DMEM. Viable cells were inoculated into 96-well plates and incubated for 48 h.[19] They were exposed for 24 h to free ATC, PCL-NC loaded with ATC, or SLN loaded with ATC, at concentrations in the range 0.1 to 1.2 mg/mL. The quantities of viable cells were determined after incubation in the presence of MTT for 2 h at 37 °C, by measuring the MTT converted to purple formazan, using a plate reader at 630 nm. The absorbance values were converted into percentages of viable cells, and the results were analyzed using ANOVA (with the Tukey–Kramer post-hoc test and $p < 0.05$).[24]

2.11. Preparation of Hydrogels Formulations Containing Free and Encapsulated ATC

The gels without the nanocarriers were prepared according to the method described in literature with some modifications. The gelling agent (Aristoflex® AVC, 2%) was added

to an aqueous solution containing methylparaben (0.1%), propylene glycol (2%), and ATC (2%), and the mixture was kept under constant agitation in a porcelain mortar until a gel was formed. The gels were then left to stabilize for 24 h. Gels containing the nanocarriers were prepared by substituting the water with the suspensions containing ATC. The final concentration of ATC in the gels was 20 mg/g of hydrogel. The gels were stored in flasks at ambient temperature and the ATC contents of the formulations were determined as a function of time.[25] Aristoflex® AVC was chosen as the gelification agent due to its ease of preparation, without requiring any previous heating or neutralization steps.

2.12. *In Vitro* Release and Permeation Studies

The *in vitro* release was studied using two-compartment system, separated by a cellulose membrane with 1 kDa MWCO. The system was maintained under constant gentle agitation and sink conditions.[26] The samples tested were: solution of free ATC (2%); PCL-NC:ATC suspension (2%); SLN:ATC suspension (2%). The *in vitro* permeation studies were performed using vertical Franz diffusion cells with a diffusional area of 1.76 cm^2 and an acceptor compartment volume of 7.0 mL.[27] The diffusion cells were assembled with nitrocellulose membranes (0.05 μm pore size) impregnated with isopropyl miristate in order to simulate the stratum corneum hydrophobicity.[28] maintained in contact with the acceptor compartment, under magnetic agitation (450 rpm). The samples tested were: gel containing free ATC (2%); gel containing PCL-NC:ATC (2%); and gel containing SLN:ATC (2%). Samples were placed in the compartment above the membrane and 1 mL aliquots were collected from the acceptor compartment at hourly intervals, during 8 h,[29,30] for analysis using the HPLC procedure described above. The data were expressed as the cumulative amounts of permeated ATC, as a function of time, and were analyzed using Eq. (2):

$$J = P \cdot Cd \tag{2}$$

where J is the flux of ATC through the membrane, P is the permeability coefficient, and Cd is the concentration of the drug used in the donor compartment.[31]

The Higuchi mathematical model was employed to analysis the ATC release mechanism from formulations. This model regards that the mechanism of drug release is dependent on the square root of time, and follows Fick's Law.[32] The Higuchi model can be described by following Eq. (3):

$$ft = K_H\sqrt{t} \tag{3}$$

where ft is the drug fraction released at a time t, and K_H is the kinetic constant.

2.13. Rheological Measurements

Rheological measurements were performed using a Haake RheoStress 1 rheometer (Thermo-Haake, Germany) with plate–plate geometry (plate diameter 20 mm). The hydrogel formulations were submitted to continuous variation of shear rate from 0 to 300 s^{-1}, and the resulting shear stress was measured. The tests were performed in triplicate ($n = 3$) at a constant temperature (25 ± 1 °C) maintained by a thermostatically-controlled water bath. The rheological profile of the hydrogel formulations was evaluated from curves obtained by plotting the shear stress (Pa) as a function of shear rate (s^{-1}).[33,34]

The thixotropic behavior of the formulations was evaluated by calculating the hysteresis loop, i.e., the area enclosed by the up and down curves.[35]

2.14. Statistical Analysis

The data were expressed as means ± standard deviations ($n = 6$). The results were analyzed by one-way ANOVA with the Tukey-Kramer post-hoc test, using a significance level of $p < 0.05$.

3. RESULTS AND DISCUSSION

3.1. Characterization of the PCL-NC and SLN Suspensions

The two nanocarrier systems were prepared for use with the model drug ATC in its neutral form. After preparation, the systems were characterized in terms of average diameter, polydispersion, pH, and morphology. In a previous study, characterization of the PCL-NC formulation revealed an encapsulation efficiency of 70% of lidocaine, an amino-amide type local anesthetic as ATC.[16] The initial characteristics of the suspensions are described in Table I.

The results showed that the average diameters and polydispersities of the suspensions containing ATC were compatible with those commonly found for colloidal suspensions. The slightly elevated pH values were due to the basicity of ATC. The polydispersity index values were below 0.2 for both suspensions, indicative of a homogeneous particle diameter distribution.[19,21] The average particle diameter was greater for the PCL-NC than for the SLN, which could be explained by the structure of the NC and the large amount of polymer used in the formulation, compared to the amount of lipid employed in the SLN. Preliminary work has shown that the average particle diameter increases when greater amounts of polymer are used, due to the increased viscosity of the organic phase.[16]

TEM micrographs obtained for the PCL-NC and SLN systems containing ATC are shown in Figure 1, together

Table I. Values of mean diameter (nm), polydispersity, and pH for suspensions of PCL-NC and SLN loaded with ATC.

Suspension	Mean diameter ± SD; (polydispersity index)	pH ± SD
PCL-NC:ATC	445.5 ± 2.1 (0.068 ± 0.005)	8.1 ± 1.2
SLN:ATC	249.9 ± 2.2 (0.113 ± 0.008)	7.9 ± 0.9

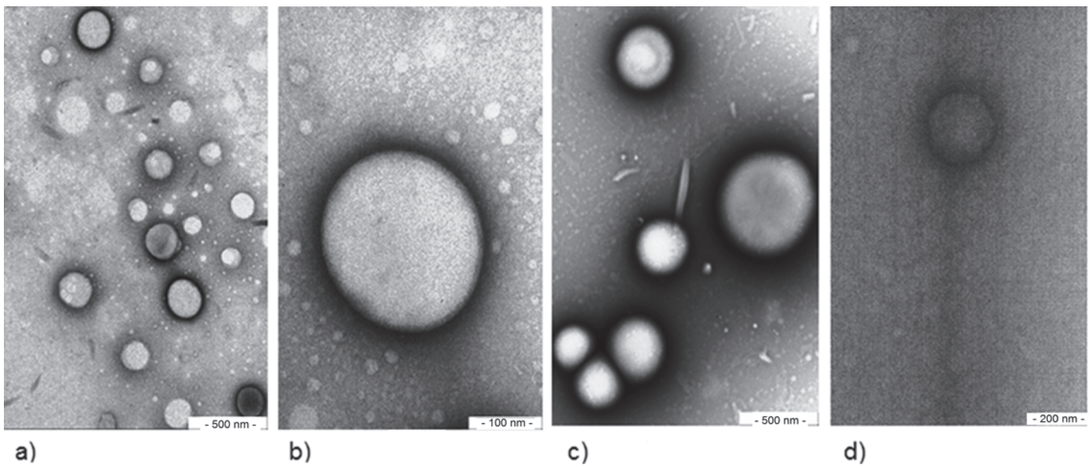

Figure 1. Transmission electron microscope images of (a–b) PCL-NC:ATC and (c–d) SLN:ATC, at magnifications of ×50,000 and ×200,000, respectively. The bars indicate the scales of the images.

with the size distributions determined by the PCS technique. The nanoparticles were spherical shape with diameters in the range 300–500 nm (Figs. 1(a–d)). These sizes were consistent with the polydispersity indices and the values obtained with the PCS technique.

Encapsulation efficiencies of 78.1% and 65.7% were obtained for the PCL-NC and SLN, respectively. This difference could be explained by a greater affinity of ATC for the oily nucleus of the PCL-NC than for the lipid used to produce the SLN, as well as by the structural characteristics of the nanoparticles. The PCL-NC are core–shell structure, while the SLN have a matrix-like structure, and studies have shown that core–shell nanoparticles are able to encapsulate hydrophobic drugs more efficiently than matrix-based nanoparticles.[36]

3.2. Stability of the Suspensions

The stability of the formulations was determined from measurements of particle diameter, polydispersity index, and pH immediately after preparation and during 120 days of storage at room temperature. Measurements of mean diameter and polydispersion provide an indication of the stability of a colloidal suspension. The size distribution of the particles is given by the polydispersity index, with values below 0.2 usually being indicative of stable suspensions.[36]

The diameters of particles in the two suspensions analyzed remained almost constant throughout the period of 120 days, indicating that stability was maintained and that there was no formation of aggregates. Similar results have been reported previously for the size stability of nanoparticles.[9,37] Over time, there were changes in polydispersion, although neither formulation showed PI values greater than 0.2 during the trial period (data not shown).

There was a reduction in pH values of both suspensions, in agreement with earlier work.[37] Due to the buffering effect of the free drug, the pH remained close to the pKa of ATC (7.8); hydrolysis of the polymer or lipid resulted in a shift in equilibrium from the neutral to the ionized form, changing the initial values of pH. In this way, both formulations showed satisfactory colloidal stability parameters and PCL-NC with higher encapsulation efficiency of ATC.

3.3. DSC Analysis

The nanoparticles and materials used in the preparation were investigated in terms of their glass transition and melting temperatures. Figure 2 shows the DSC curves obtained for ATC, the PCL polymer, the physical mixture (ATC + PCL), and the PCL-NC with and without ATC. Figure 3 shows the DSC curves obtained for ATC, glyceryl tripalmitate (TP), the physical mixture (ATC + TP), and the SLN with and without ATC.

ATC showed an endothermic peak at 68 °C that corresponded to the melting point of the drug. For the PCL, there was a thermal transition peak at 58.6 °C due to melting of the crystalline phase, consistent with previous work.[38] The PCL-NC showed an endothermic peak at around 55 °C, indicating that the manufacturing process increased the heterogeneity of the crystal polymer and produced less perfect structures with lower melting temperatures.[39] In the case of the PCL-NC:ATC, there was a displacement of the endothermic peak. This decrease in melting temperature was indicative of an interaction between the drug and the carrier system that altered the crystal lattice. The endothermic melting point peak of ATC was not observed in the PCL-NC curve, suggesting that the drug was dispersed inside the NC or on their surfaces.[39] To investigate this hypothesis, the thermal behavior of a physical mixture (PCL and ATC) was also evaluated. The curve showed overlapping endothermic peaks for the polymer and the drug. Thus, even if the drug was in crystalline form, peak overlap could have

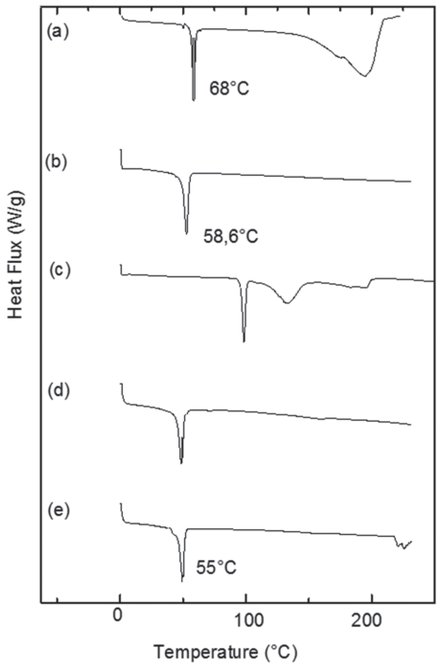

Figure 2. DSC curves obtained for (a) ATC, (b) PCL polymer, (c) ATC + PCL physical misture, (d) PCL-NC and (e) PCL-NC:ATC.

prevented detection of the ATC peak in the curves for the PCL-NC:ATC.

Glyceryl tripalmitate showed an endothermic peak at 64.0 °C due to fusion of the lipid, involving the β form, in agreement with the literature.[3] Two endothermic peaks were observed for the SLN, at 45.7 and 61.9 °C, due to the presence of the PVA surfactant. The presence of a surfactant alters the lipid packing arrangement, with the formation of new polymorphic forms. It has been suggested that the PVA immobilizes lipid molecules in the interfacial region, preventing reestablishment of the β form.[21] The peak at around 45 °C could be attributed to the presence of coalescent lipid particles that crystallized by heterogeneous nucleation (α form), while the peak at around 61 °C corresponded to the fusion temperature of tripalmitin. Similar results have been obtained previously for SLN composed of tripalmitin.[3] In the case of the SLN:ATC, an endothermic peak occurred at 60.2 °C. This decrease in the fusion temperature was suggestive of interaction between the drug and the carrier system, which altered the crystallization and fusion of the lipid. In addition, ATC endothermic fusion peak was not observed in the curve for SLN:ATC, indicating that the drug was dispersed in the interior or on the surface of the nanoparticles. The curve obtained for the physical mixture (TP and ATC) showed the presence of endothermic peaks for the lipid as well as the drug. This confirmed that the technique was able to detect the peaks corresponding to ATC and TP, and that in the case of the SLN:ATC, the drug was dispersed in the lipid matrix.

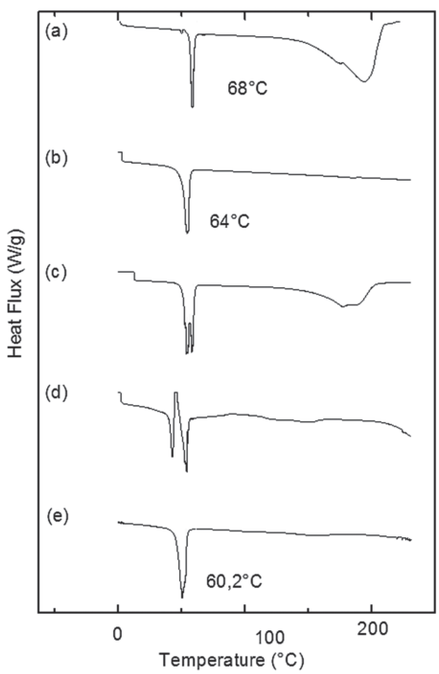

Figure 3. DSC curves obtained for (a) ATC, (b) TP, (c) ATC + TP physical mixture, (d) SLN, and (e) SLN:ATC.

The incorporation of nanoparticles in the gels did not alter the structures of the same indicating that the vehicle was suitable for the placement of nanoparticles (data not shown).

3.4. Cellular Viability Assays

The MTT reduction test was used to determine cellular viability. Figure 4 presents the results obtained with mouse 3T3 fibroblasts incubated with free ATC, PCL-NC:ATC, and SLN:ATC (0.1–1.2 mg/mL). Empty nanoparticles were also tested.

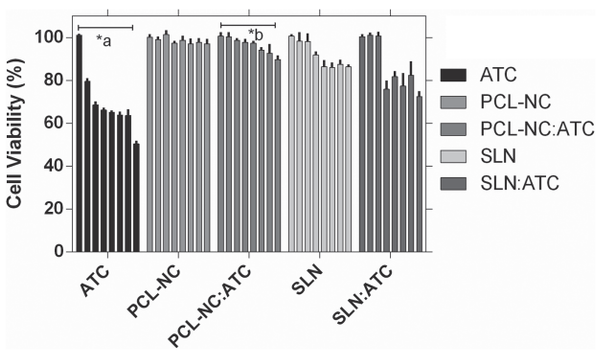

Figure 4. Cellular viability determined using the MTT test after exposure of Balb-c 3T3 cells to free ATC and ATC incorporated in PCL-NC and SLN suspensions ($n = 12$). Data reported as mean ± SD. $^*p < 0.05$, one-way ANOVA with the Tukey-Kramer post-hoc test ($^*a$—ATC vs. PCL-NC:ATC or SLN:ATC; $^*b$—PCL-NC:ATC vs. SLN:ATC).

It is possible that the loaded polymers, lipids, and other components of the formulations could present some degree of interaction with cell membranes.[40] However, at the concentrations tested, exposure to PCL-NC and SLN did not affect cellular viability. A protective effect was observed for treatment using ATC associated with the PCL-NC and SLN, which can be explained by the lower availability of the drug due to its modified release from the nanoparticles. Exposure of the cells to the free drug reduced cellular viability by around 50%, while exposure to PCL-NC:ATC and SLN:ATC promoted cell viability around to 90% and 75%, respectively, at the highest concentration tested (1.2 mg/mL). Similar results have been reported for poly-lactide-co-glycolide (PLGA) nanospheres containing ropivacaine, alginate nanoparticles containing bupivacaine, and PCL nanospheres containing lidocaine, where encapsulation the drug into the nanocarriers resulted in good cellular viability.[19,41] The ATC encapsulated in alginate/chitosan nanoparticles and PEG-PCL nanocapsules was also investigated at the same ATC concentration. The results showed the nanoencapsulation was able to improve cellular viability compared with free drug, and this effect was related with drug encapsulation efficiency.[9] The more encapsulated drug, lower the side effect of the formulation. Thus, both nanoparticulated systems (PCL-NC and SLN) promoted elevated cellular viability percentages than free drug, confirming the systems have high encapsulation efficiency and modified release profile, being PCL-NC system provided higher values compared with SLN system.

3.5. *In Vitro* Release Kinetics

The release of ATC was investigated using free ATC, PCL-NC:ATC, and SLN:ATC (Fig. 5). In the system described above, only free ATC molecules were able to traverse the cellulose acetate membrane, while the nanoparticles were unable to pass through the membrane. It was therefore possible to evaluate the interactions between ATC and the nanocarriers. Samples were collected from the acceptor compartment for quantification of ATC, and the results were expressed as the percentage of ATC released.

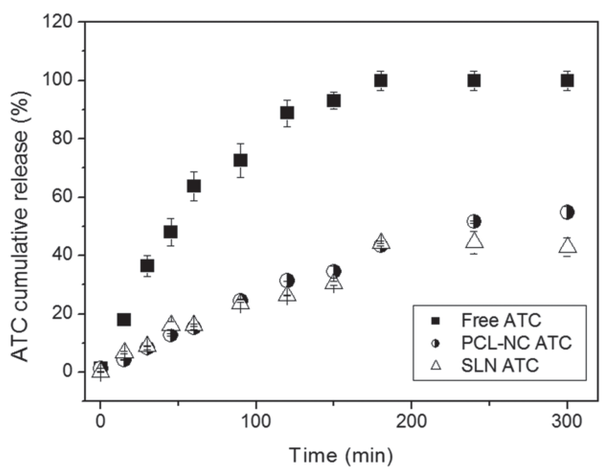

Figure 5. Cumulative release of ATC, free or in suspensions of SLN or PCL-NC, at ambient temperature ($n = 3$).

The release curves showed that there was complete (100%) release of free ATC after 300 min, with 50% release ($t_{50\%}$) after 45 min, while the PCL-NC:ATC and SLN:ATC suspensions showed $t_{50\%}$ values of 400 and 300 min, respectively, demonstrating that both formulations were able to modify the ATC release profile. These differences in the release profiles could be attributed to the different structures of the nanoparticles and release process.[32,42]

Due to the lipophilic nature of neutral ATC, the drug showed a high affinity for the hydrophobic matrices, which was reflected in the encapsulation efficiencies. The drug was released more slowly from the SLN, compared to free ATC, although the difference was smaller than obtained for PLC-NC:ATC. This can be explained by greater interaction of neutral ATC with the oily nucleus and polymeric wall of the PLC-NC, so that there was greater restriction of ATC release from the vesicular structure.

The Higuchi model was used to analyze the release profiles in order to identify the mechanism involved. The rate constants (k) and correlation coefficients (r) were calculated using linear regression. Values of k of 5.85 min^{-1} ($r = 0.993$) and 8.32 min^{-1} ($r = 0.997$) were obtained for PCL-NC:ATC and SLN:ATC, respectively. These values indicated that the release of ATC occurred according to a Fickian diffusion mechanism. This kind of release mechanism has been reported previously for PCL nanocapsules loaded with lidocaine.[19]

3.6. Hydrogels Formulations

After characterization, the nanoparticle suspensions were incorporated into hydrogels formulations composed of Aristoflex® AVC. The semi-solid formulations containing free or encapsulated ATC were evaluated in terms of their appearance, color and odor, 24 h after preparation and then after 30 days. All the formulations showed surfaces that were smooth, shiny, and homogeneous, indicating that the vehicle was suitable for the preparation of formulations containing ATC. An important point is that the products containing nanoparticles did not show the gelatine-like appearance common to formulations based on the Aristoflex® AVC polymer due to the presence of surfactants in the nanoparticle suspensions.

The formulations stored at ambient temperature (25 °C) showed no changes in terms of color, odor, and appearance during the 30 days of the trial. The values obtained for the average diameter and polydispersity index of the suspensions incorporated in Aristoflex AVC® are provided in Table II.

In the case of the SLN:ATC gel, there were increases in the average diameter and polydispersion of the nanoparticles after incorporation of the suspensions in the vehicle,

Table II. Average diameter, polydispersity index, and zeta potential of nanoparticles containing ATC incorporated in Aristoflex AVC®.

Formulation	Average diameter (nm)	Polydispersity
Gel PCL-NC:ATC 2%	463.2 ± 24.7	0.190 ± 0.013
Gel SLN:ATC 2%	315.3 ± 20.1	0.206 ± 0.009

compared to the values obtained for the suspensions. It is possible that interaction between the structure of the gel and the nanoparticles resulted in progressive aggregation of the particles.[43] For the PCL-NC:ATC gel formulation, there was no substantial change in the average particle diameter, compared to the values obtained for the suspension, indicating that there were no changes in the physico-chemical characteristics of this nanoparticulate system after incorporation in the gel.

The permeation profiles of the different formulations were characterized under sink conditions. The results obtained were expressed in terms of the cumulative amount of ATC permeated as a function of time (Fig. 6). The slope of the straight line for the period 1–8 h represented the permeation flux of ATC through the membrane, and the intersection with the *x*-axis indicated the time required for the initiation of permeation (the lag time),[44] as shown in Table III. It is important to note that *sink* conditions were maintained in the diffusion cells throughout these experiments.

According Figure 6, a slower permeation profile was observed at the first two hours for the gel containing free ATC compared to the gels containing nanoparticles. The use of IPM as a simulant of the hydrophobicity of the stratum corneum[28] could create two phases (hydrophilic gel and hydrophobic layer) partitioning the drug. If comparing the formulations containing the PCL nanocapsules or SLN, the initial profile changes because, although they are in the same type of gel, the nanoparticles can cross

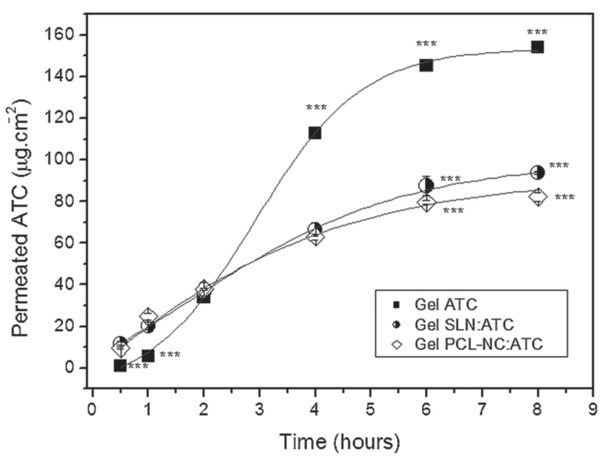

Figure 6. Permeation profiles of ATC for different gel formulations based on Aristoflex® AVC. Data presented as means and standard deviations ($n = 3$). $^{***}p < 0.05$, one-way ANOVA with the Tukey-Kramer post-hoc test.

Table III. Permeation parameter values obtained for permeation of different ATC gels through a cellulose acetate membrane (period: 1–8 h; 20 mg ATC/g of gel).

Formulation	Flux ($\mu g/cm^2/h$)*	Lag time (h)	Permeability coefficient ($\times 10^{-3} cm^2/h$)	Quantity of ATC permeated ($\mu g/cm^2$) (8 h)**
ATC gel	82.56 ± 1.41**	0.670 ± 0.013**	3.57	154.06 ± 2.68
SLN:ATC gel	41.52 ± 0.66**	0.220 ± 0.078	1.94	93.86 ± 1.17
PCL-NC: ATC gel	35.68 ± 1.98**	0.121 ± 0.044	1.97	82.31 ± 3.91

Notes: *Calculated on the linear portion of the curve; **Statistically significant values ($p < 0.05$; one-way ANOVA with the Tukey-Kramer post-hoc test).

the IPM layer, disperse themselves and increase drug penetration.[45,46] However, the gel containing free drug must initially saturate the IPM layer after being found in the receptor medium (therefore, the time required for permeation of high ATC concentrations is slower). After this period (2 hours), it was possible to observe the effect of prolonged release promoted by the nanoparticulate system. Therefore, the permeation profile of the gel containing the free drug becomes faster than the permeation profile of the gels containing nanoparticles.

Application of the Higuchi mathematical model resulted in satisfactory fits to the release profiles (ATC gel: $r^2 = 0.976$; PCL-NC:ATC gel: $r^2 = 0.999$; SLN:ATC gel: $r^2 = 0.997$). This showed that the mechanism of release of free and encapsulated ATC in the semi-solid formulations was due to a diffusion process that could be described by Fick's First Law, since the drug is the component which presents possibly a dual diffusion:
(i) from nanoparticles in direction to the gel matrix and
(ii) from the polymeric gel-base until the medium, explaining the slow permeation and lower flux values regarding to ATC gel and ATC-nano emulsions.

It can be seen from Table III that the formulation containing 2% free ATC showed the highest permeation value (82.56 ± 0.35 $\mu g/cm^2/h$), lag time (0.670 ± 0.013 h), and permeability coefficient (0.00357 cm^2/h). This formulation therefore provided permeation of a greater quantity of ATC through the membrane, while the time required for initiation of permeation was significantly longer, compared to the other formulations ($p < 0.05$).

Much lower flux values were obtained for the formulations containing nanoparticles with ATC. There was a statistically significant difference between these two formulations in terms of the flux, which was lowest for the PCL-NC:ATC 2% gel, while no statistically significant difference was observed for the lag time. These results were in agreement with the release profiles of the suspensions of PCL-NC and SLN containing ATC.

The slower release of ATC from the PCL-NC than from the SLN was related to the efficiency with which ATC

was encapsulated in these systems, with higher encapsulation efficiency leading to slower release. This pattern was repeated for the permeation of ATC in the semi-solid preparations, with the formulation containing PCL-NC:ATC presenting the lowest flux and the smallest permeability coefficient.

According to the literature, nanoparticle systems exhibit biphasic behavior, with an initial rapid release of the active agent (a burst effect), followed by a period of slower release.[47] The initial release phase can be attributed to the presence of the active agent in its free form, while the second phase corresponds to diffusion of the active substance following degradation of the nanoparticle matrix. This process of diffusion is governed by the coefficient of partition of the agent between the polymer or lipid and the external aqueous medium.[47]

The gel containing free ATC showed faster release, compared to the formulations containing the nanoencapsulated drug for both the flux and the total amount released ($p < 0.05$), although there was a longer lag time, compared to the formulations containing nanoparticles. The shorter lag time for the nanoparticle formulations could be explained by the "burst effect" associated with the presence of free ATC that had not been encapsulated,[47] and the lower fluxes could be attributed to the modification of the release profile induced by the presence of the nanoparticles.

In terms of clinical applications, the flux values exhibited by the formulations of ATC encapsulated in nanoparticles suggested the ability to provide a more prolonged anesthetic effect of ATC. The permeation kinetics data showed that the lag times were shorter for these formulations, which in clinical practice would help to minimize the time delay before onset of the anesthetic effect.

3.7. Rheological Measurements

An important characteristic of semi-solid systems is that they preserve their shape when not under pressure, but flow or deform when submitted to an external force. Since conventional nanoparticle suspensions present low viscosity, alternative dosage forms (such as hydrogels) are required when a topical application is desired.[34] However, the rheological properties of the final formulation need to be evaluated, because the components of the gel and the suspension can interact and affect the consistency of the resulting hydrogel.[34] The rheological behaviors of the two different hydrogels containing SLN and PCL-NC, together with those of the control formulations (base gel and free ATC in the base gel), are illustrated in the flow curves profiles shown in Figure 7.

The rheograms reflected non-Newtonian pseudoplastic flows, where the shear rate increased with increasing shear stress.[35] After achieving the maximum supported shear stress, the formulations started to flow and their viscosity decreased. These characteristics have been

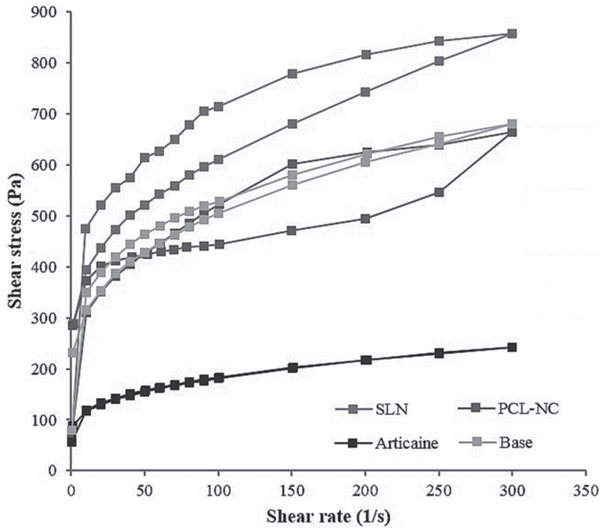

Figure 7. Shear stress as a function of shear rate for the two different hydrogels containing SLN and PCL-NC, and the control formulations (base gel and free ATC in the base gel). The upper and lower curves correspond to ascending and descending measurements, respectively, for each formulation. SD values were below 5%.

demonstrated previously for hydrogel-based formulations containing solid lipid nanoparticles and nanostructured lipid carriers.[34, 48]

Figure 7 also reveals a high shear stress values with the increase of shear rate for the SLN and PCL-NC hydrogels, reflecting greater viscosity of the nanoparticle formulations. It has been suggested previously that this could be indicative of good storage stability of semi-solid formulations, as well as improved spreadability.[49]

Another property related to pseudoplastic systems is thixotropy, which is a time-dependent decrease in viscosity under shear stress, followed by a gradual recovery when the stress is removed.[35] This is a common characteristic of formulations containing nanoparticles.[48] As calculated from Figure 7 the SLN (22,090.23 $Pa \cdot s^{-1}$) and PCL-NC (19,554.99 $Pa \cdot s^{-1}$), hydrogels both presented thixotropy, while thixotropic behavior was not observed for the base gel or the free ATC formulation. These observations could also be related to the presence of lipids in the formulations, which helps to ensure good spreadability in topical applications.[34, 48] Thixotropic properties contribute to increased retention times of topically applied formulations, leading to better therapeutic efficacy,[35] which was an essential consideration in the case of the hydrogels developed in the present study.

4. CONCLUSIONS

This work provides new information concerning the preparation and characterization of nanoparticles and semi-solid formulations containing the ATC local anesthetic. Good encapsulation efficiencies were achieved, with values of

around 78% for PCL-NC and 65% for SLN. In stability trials, measurements of colloidal parameters demonstrated that suspensions of these nanocarrier systems containing ATC remained stable for a period of 120 days. The encapsulation of ATC result higher cellular viability values for the nanosystem formulations, compared to free ATC, which could be explained by the efficiency of encapsulation of the drug, resulting in smaller amounts of free ATC. The profile of ATC release was slower and more sustained for the PCL-NC and SLN formulations, compared to free ATC.

Semi-solid formulations incorporating ATC, either free or encapsulated in the nanocarriers, were prepared using Aristoflex® AVC gel. No changes in visual appearance of the formulations were noted at time zero and after 30 days, confirming the suitability of this vehicle. Determination of the average diameter and polydispersion of the nanoparticles incorporated in the gel showed that there were no changes in the colloidal parameters and that the vehicle did not alter the stability of the suspensions of nanoparticles containing ATC. Rheological evaluation showed that the SLN and PCL-NC hydrogel formulations presented non-Newtonian pseudoplastic flows with thixotropy. In clinical practice, this should be reflected in better stability, increased retention time at the application site, and improved spreadability. The results of *in vitro* permeation experiments employing the semi-solid formulations demonstrated that the lag time was shorter for the preparations containing nanoparticles, compared to the preparation containing free ATC, and that the flow of ATC through the membrane was slower for the nanoparticle systems. The formulation containing ATC encapsulated in PCL-NC showed the best permeation characteristics. This study opens perspectives for the future use of nanoparticulate carrier systems for the ATC local anesthetic, envisaging their infiltrative and/or topical use in clinical practice.

Disclosure of Interest

The authors report no conflicts of interest.

Acknowledgments: This work was supported by the São Paulo Research Foundation (FAPESP) under grants #2010/11097-7 and #2010/18529-0; National Counsel of Technological and Scientific Development (CNPq); and FUNDUNESP.

References and Notes

1. C. Preetz, A. Rübe, I. Reiche, G. Hause, and K. Mäder, *Nanomedicine Nanotechnol. Biol. Med.* 4, 106 (**2008**).
2. E. Marin, M. I. Briceño, and C. Caballero-George, *Int. J. Nanomedicine* 8, 3071 (**2013**).
3. T. Helgason, T. S. Awad, K. Kristbergsson, D. J. McClements, and J. Weiss, *J. Colloid Interface Sci.* 334, 75 (**2009**).
4. S. Doktorovova, E. B. Souto, and A. M. Silva, *Eur. J. Pharm. Biopharm.* 87, 1 (**2014**).
5. S. F. Malamed, Handbook of Local Anesthesia, 6th edn., Mosby, Missouri (**2012**), p. 66.
6. E. A. Shipton, *Anesthesiol. Res. Pract.* 2012, Article ID: 546409 (**2012**).
7. M. Diaz, *TeamWork* 2, 28 (**2009**).
8. K. Paxton and D. E. Thome, *Dent. Clin. North Am.* 54, 643 (**2010**).
9. N. F. S. de Melo, E. V. R. Campos, C. M. Gonçalves, E. de Paula, T. Pasquoto, R. de Lima, A. H. Rosa, and L. F. Fraceto, *Colloids Surf. B Biointerfaces* 121, 66 (**2014**).
10. C. B. da Silva, F. C. Groppo, C. P. dos Santos, L. Serpe, M. Franz-Montan, E. de Paula, J. Ranali, and M. C. Volpato, *Br. J. Oral Maxillofac. Surg.* 54, 295 (**2016**).
11. P. D. Ribeiro, M. G. Sanches, and T. Okamoto, *Anesth. Prog.* 50, 169 (**2003**).
12. T. Batinac, V. Sotošek Tokmadžić, V. Peharda, and I. Brajac, *J. Dermatol.* 40, 522 (**2013**).
13. R. Alvarez-Román, A. Naik, Y. N. Kalia, R. H. Guy, and H. Fessi, *J. Controlled Release* 99, 53 (**2004**).
14. S. S. Bharate and R. A. Vishwakarma, *Expert Opin. Drug Deliv.* 10, 1239 (**2013**).
15. A. K. Santis, Z. M. F. de Freitas, E. Ricci-Junior, L. de Brito-Gitirana, L. B. Fonseca, and E. P. Santos, *Drug Dev. Ind. Pharm.* 39, 1098 (**2013**).
16. E. V. R. Campos, N. F. S. de Melo, E. de Paula, A. H. Rosa, and L. F. Fraceto, *J. Colloid Sci. Biotechnol.* 2, 106 (**2013**).
17. N. F. S. de Melo, E. V. R. Campos, E. de Paula, A. H. Rosa, and L. F. Fraceto, *J. Colloid Sci. Biotechnol.* 2, 146 (**2013**).
18. D. B. Larsen, H. Parshad, K. Fredholt, and C. Larsen, *Int. J. Pharm.* 232, 107 (**2002**).
19. E. V. Ramos Campos, N. F. Silva de Melo, V. A. Guilherme, E. de Paula, A. H. Rosa, D. R. de Araújo, and L. F. Fraceto, *J. Pharm. Sci.* 102, 215 (**2013**).
20. J. L. de Oliveira, E. V. R. Campos, C. M. Gonçalves da Silva, T. Pasquoto, R. Lima, and L. F. Fraceto, *J. Agric. Food Chem.* 63, 422 (**2015**).
21. C. Vitorino, F. A. Carvalho, A. J. Almeida, J. J. Sousa, and A. A. C. C. Pais, *Colloids Surf. B Biointerfaces* 84, 117 (**2011**).
22. N. F. Silva De Melo, D. R. De Araújo, R. Grillo, C. M. Moraes, A. P. De Matos, E. de Paula, A. H. Rosa, and L. F. Fraceto, *J. Pharm. Sci.* 101, 1157 (**2012**).
23. M. dos S. Silva, D. S. Cocenza, R. Grillo, N. F. S. de Melo, P. S. Tonello, L. C. de Oliveira, D. L. Cassimiro, A. H. Rosa, and L. F. Fraceto, *J. Hazard. Mater.* 190, 366 (**2011**).
24. R. de Lima, L. O. Feitosa, C. R. Maruyama, M. A. Barga, P. C. Yamawaki, I. J. Vieira, E. M. Teixeira, A. C. Corrêa, L. H. C. Mattoso, and L. F. Fraceto, *Int. J. Nanomedicine* 7, 3555 (**2012**).
25. P. Batheja, L. Sheihet, J. Kohn, A. J. Singer, and B. Michniak-Kohn, *J. Controlled Release* 149, 159 (**2011**).
26. A. Paavola, J. Yliruusi, Y. Kajimoto, E. Kalso, T. Wahlström, and P. Rosenberg, *Pharm. Res.* 12, 1997 (**1995**).
27. J. P. Venter, D. G. Müller, J. du Plessis, and C. Goosen, *Eur. J. Pharm. Sci.* 13, 169 (**2001**).
28. R. Jantharaprapap and G. Stagni, *Int. J. Pharm.* 343, 26 (**2007**).
29. M. Franz-Montan, D. Baroni, G. Brunetto, V. R. V. Sobral, C. M. G. da Silva, P. Venâncio, P. W. Zago, C. M. S. Cereda, M. C. Volpato, D. R. de Araújo, E. de Paula, and F. C. Groppo, *J. Liposome Res.* 25, 11 (**2015**).
30. M. Franz-Montan, C. M. S. Cereda, A. Gaspari, C. M. G. da Silva, D. R. de Araújo, C. Padula, P. Santi, E. Narvaes, P. D. Novaes, F. C. Groppo, and E. de Paula, *J. Liposome Res.* 23, 54 (**2013**).
31. S. Nicoli, P. Colombo, and P. Santi, *AAPS J.* 7, E218 (**2005**).
32. J. Siepmann and F. Siepmann, *Int. J. Pharm.* 364, 328 (**2008**).
33. D. S. Jones, M. S. Lawlor, and A. D. Woolfson, *J. Pharm. Sci.* 92, 995 (**2003**).
34. E. B. Souto, S. A. Wissing, C. M. Barbosa, and R. H. Müller, *Eur. J. Pharm. Biopharm.* 58, 83 (**2004**).
35. C. H. Lee, V. Moturi, and Y. Lee, *J. Control. Release Off. J. Control. Release Soc.* 136, 88 (**2009**).

36. C. E. Mora-Huertas, H. Fessi, and A. Elaissari, *Int. J. Pharm.* 385, 113 **(2010)**.
37. N. F. S. de Melo, R. Grillo, V. A. Guilherme, D. R. de Araujo, E. de Paula, A. H. Rosa, and L. F. Fraceto, *Pharm. Res.* 28, 1984 **(2011)**.
38. V. K. Khatiwala, N. Shekhar, S. Aggarwal, and U. K. Mandal, *J. Polym. Environ.* 16, 61 **(2008)**.
39. S. Freiberg and X. X. Zhu, *Int. J. Pharm.* 282, 1 **(2004)**.
40. N. Nafee, M. Schneider, U. F. Schaefer, and C.-M. Lehr, *Int. J. Pharm.* 381, 130 **(2009)**.
41. R. Grillo, N. F. S. de Melo, D. R. de Araújo, E. de Paula, A. H. Rosa, and L. F. Fraceto, *J. Drug Target.* 18, 688 **(2010)**.
42. S. Das, W. K. Ng, P. Kanaujia, S. Kim, and R. B. H. Tan, *Colloids Surf. B Biointerfaces* 88, 483 **(2011)**.
43. D. Milão, M. T. Knorst, W. Richter, and S. S. Guterres, *Pharm.-Int. J. Pharm. Sci.* 58, 325 **(2003)**.
44. D. Kaushik, A. Costache, and B. Michniak-Kohn, *Int. J. Pharm.* 386, 42 **(2010)**.
45. F. Knorr, J. Lademann, A. Patzelt, W. Sterry, U. Blume-Peytavi, and A. Vogt, *Eur. J. Pharm. Biopharm.* 71, 173 **(2009)**.
46. L. A. D. Silva, S. F. Taveira, E. M. Lima, and R. N. Marreto, *Braz. J. Pharm. Sci.* 48, 811 **(2012)**.
47. E. Cauchetier, M. Deniau, H. Fessi, A. Astier, and M. Paul, *Int. J. Pharm.* 250, 273 **(2003)**.
48. A. C. Silva, M. H. Amaral, E. González-Mira, D. Santos, and D. Ferreira, *Colloids Surf. B Biointerfaces* 93, 241 **(2012)**.
49. E. B. Souto and R. H. Müller, *Pharm.* 62, 505 **(2007)**.

Received: 31 March 2017. Accepted: 6 July 2017.